Received: 17 February 2021 | Revised: 18 April 2021 | Accepted: 20 April 2021

DOI: 10.1002/rcm.9113

RESEARCH ARTICLE

Rapid Communications in Mass Spectrometry WILEY

The maximum carbonyl ratio (MCR) as a new index for the structural classification of secondary organic aerosol components

Yun Zhang[1] | Kai Wang[2] | Haijie Tong[3] | Ru-Jin Huang[4] | Thorsten Hoffmann[1]

[1]Department of Chemistry, Johannes Gutenberg University, Mainz, 55128, Germany

[2]Key Laboratory of Plant-Soil Interactions of MOE, College of Resources and Environmental Sciences, National Academy of Agriculture Green Development, China Agricultural University, Beijing, 100193, China

[3]Department of Civil and Environmental Engineering, The Hong Kong Polytechnic University, Kowloon, Hong Kong, China

[4]State Key Laboratory of Loess and Quaternary Geology, Key Laboratory of Aerosol Chemistry and Physics, Institute of Earth Environment, Chinese Academy of Sciences, Xi'an, 710061, China

Correspondence
T. Hoffmann, Department of Chemistry, Johannes Gutenberg University, 55128 Mainz, Germany.
Email: t.hoffmann@uni-mainz.de

Funding information
German Federal Ministry of Education and Research, Grant/Award Number: 01LK1602D; Deutsche Forschungsgemeinschaft, Grant/Award Numbers: HO 1748/19-1, HO 1748/20-1; National Natural Science Foundation of China (NSFC), Grant/Award Number: 41925015; Max Planck Society

Rationale: Organic aerosols (OA) account for a large fraction of atmospheric fine particulate matter and thus are affecting climate and public health. Elucidation of the chemical composition of OA is the key for addressing the role of ambient fine particles at the atmosphere–biosphere interface and mass spectrometry is the main method to achieve this goal.

Methods: High-resolution mass spectrometry (HRMS) is on its way to becoming one of the most prominent analytical techniques, also for the analysis of atmospheric aerosols. The combination of high mass resolution and accurate mass determination allows the elemental compositions of numerous compounds to be easily elucidated. Here a new parameter for the improved classification of OA is introduced – the maximum carbonyl ratio (MCR) – which is directly derived from the molecular composition and is particularly suitable for the identification and characterization of secondary organic aerosols (SOA).

Results: The concept is exemplified by the analysis of ambient OA samples from two measurement sites (Hyytiälä, Finland; Beijing, China) and of laboratory-generated SOA based on ultrahigh-performance liquid chromatography (UHPLC) coupled to Orbitrap MS. To interpret the results, MCR–Van Krevelen (VK) diagrams are generated for the different OA samples and the individual compounds are categorized into specific areas in the diagrams. The results show that the MCR index is a valuable parameter for representing atmospheric SOA components in composition and structure-dependent visualization tools such as VK diagrams.

Conclusions: The MCR index is suggested as a tool for a better characterization of the sources and the processing of atmospheric OA components based on HRMS data. Since the MCR contains information on the concentration of highly electrophilic organic compounds in particulate matter (PM) as well as on the concentration of organic (hydro)peroxides, the MCR could be a promising metric for identifying health-related particulate matter parameters by HRMS.

1 | INTRODUCTION

Organic aerosols (OA) account for a large fraction (20–90%) of submicron particulate mass in the atmosphere with consequences for climate and public health.[1–5] Atmospheric OA, including primary organic aerosol particles emitted directly from sources and secondary organic aerosol (SOA) formed by oxidation of precursors in the atmosphere, originate from a wide variety of biogenic (e.g., terrestrial vegetation) and anthropogenic (e.g., biomass burning and fossil fuel combustion) sources.[6] Due to their diverse sources, various formation pathways and complex multiphase aging processes, the OA fraction is composed of thousands of different compounds, which contain various functional groups including hydroxyl, hydroperoxide, carbonyl and carboxyl groups, but also sulfur- and nitrogen-containing functional groups (organic nitrates and sulfates). The vast number of individual compounds results in a wide range of physical, chemical and toxicological properties and complicates the OA characterization; this complexity in combination with sophisticated mass spectrometric instrumentation also offers the possibility to decipher OA sources, formation pathways and the fate of OA in the atmosphere.[7–13] Thus, it is essential to develop highly efficient analytical techniques to gather detailed, compound-specific chemical information.

In the last decade, analytical methods based on high-resolution mass spectrometry (HRMS), such as Fourier transform ion cyclotron (FTICR) and Orbitrap MS, in combination with soft ionization techniques, including atmospheric pressure chemical ionization (APCI) and electrospray ionization (ESI), have been successfully applied to OA research.[7,9,11–17] HRMS benefits from two outstanding features, high mass spectrometric resolution (>40,000) and high mass accuracy (<5 ppm). As a consequence, HRMS allows the assignment of unique elemental compositions and enables the calculation of the molecular formulae for the analytes of interest even in highly complex samples, often hundreds or thousands of compounds. However, accompanying the complexity and size of the datasets, new needs and challenges arise concerning the interpretation and visualization of the HRMS results. Consequently, visualization tools like van Krevelen (VK) diagrams,[18–20] Kendrick mass defect (KMD) analysis[21,22] and carbon oxidation state (OSc)[1,15] plots were developed. Most often VK diagrams are applied, which place every assigned unique chemical formula on a two-dimensional (2D) scatterplot of H/C ratio versus O/C ratio, to sort and group the organic compounds identified by the HR mass spectra.

One obvious chemical feature which directly results from the elemental composition of the analytes is their degree of unsaturation (DU) or double-bond equivalents (DBE). The DBE represents the sum of the number of double bonds and rings in a molecule and is a well-established and helpful tool in mass spectrometry.[23,24] However, a limitation of this metric is that the DBE cannot distinguish C–C double bonds from C–O/C–S double bonds when divalent atoms (e.g., O and S) are present in the molecules. By definition of the DBE the divalent oxygen does not influence the DBE value, although obviously oxygen can also contribute to double bonds of organic molecules. Therefore, aiming towards a better structural characterization of complex organic mixtures, the aromaticity index (AI)[25] and the aromaticity equivalent (Xc)[24] have been introduced in recent years. The advantage of the AI and the Xc over the simple use of the DBE is that they also consider heteroatoms (O, S, and N) as contributors to the DU and that they define threshold values to quantify the aromaticity of the organic molecules. As a consequence, parameters such as the AI or Xc are beneficial for the characterization of aromatic/condensed aromatic compounds. However, for the characterization of chemical structures of typical ambient SOA compounds, the AI or the Xc is less appropriate. First of all, the majority of typical SOA components rarely contain aromatic structures, since the main gaseous SOA precursors are non-aromatic compounds.[3] Moreover, even when aromatic volatile organic compounds (VOCs) serve as SOA precursors, which can be expected in mostly anthropogenically influenced areas, their aromaticity is frequently lost during the initial oxidation steps, i.e., due to the dominant OH addition to the aromatic ring followed by rapid further oxidation steps.[26] Actually, also other structural elements influencing the DBE of SOA precursor molecules, such as C–C multiple bonds or carbon ring structures, are prone to be lost in the process of SOA formation. This is especially true for C–C double bounds, which represent the main chemical feature of biogenic VOCs (e.g., isoprene, monoterpenes, sesquiterpenes), which in turn are the most important SOA precursors on the global scale. The double bonds are preferentially attacked by atmospheric oxidants (ozone, OH and nitrate radicals) and hence tend to disappear prior to the gas-to-particle conversion of the products. Less obvious, but with similar behavior are cyclic compounds, for which ring-opening pathways yield especially low-volatility oxidation products that finally make a notable contribution to the particle phase. Therefore, in the process of SOA formation most structural elements (C=C and rings) which usually contribute to a carbon-related degree of unsaturation in organic matter disappear and are replaced by unsaturation connected with the introduced oxygen-containing functionalities.

In principle, SOA components contain oxygen atoms in the form of hydroxyl (OH), hydroperoxide (OOH) or peroxide (-OO-), carbonyl (C=O), carboxyl (COOH) and epoxide groups.[17] Obviously, the carbonyl group (C=O), in the form of an aldehyde, ketone or carboxyl group, as well as the epoxide group can contribute to the DU. In contrast, in the absence of unsaturation of a specific SOA compound (oxygen is always present in SOA), alcohol or peroxide functionalities must be present. In the context of SOA chemistry especially the latter functionality has created pronounced scientific interest, since highly oxidized multifunctional organic compounds (HOMs) are supposed to be multifunctional hydroperoxides formed via autooxidation.[27] Due to their low vapor pressure, HOMs are able to contribute to the formation of new particles in the atmosphere and thus, via their function as cloud condensation nuclei, ultimately have a major impact on the atmospheric radiation balance.[28] However, peroxide functionalities may also play an important role in health-related effects of SOA, since organic (hydro)peroxides are thought to

contribute to the formation of reactive oxygen species (ROS) by transporting oxidants on/in particles into the respiratory system.[29,30]

It is noteworthy to point out that the DU as discussed above results in distinct chemical properties. For example, both carbonyls and epoxides possess a high electrophilic reactivity. The polarized double bond in carbonyls and even more pronounced the three-membered ring in epoxides induce a high reactivity towards nucleophilic addition reactions. This reactivity enables the formation of covalent bonds between the electrophile (carbonyl/epoxide carbon) and a nucleophilic partner molecule (alcohols, other carbonyls, amines). On the one hand this reactivity is directly relevant for atmospheric heterogeneous/multiphase chemistry and the formation of higher molecular weight compounds in SOA. In other words, higher concentrations of carbonyls/epoxides cause a higher potential for condensed-phase chemistry and the formation of oligomers by homogeneous aging.[31] In contrast, low carbonyl/epoxide content together with the presence of high molecular weight compounds could indicate that condensed-phase chemistry already happened (homogeneously aged SOA). On the other hand, and probably diagnostically more valuable, is the high electrophilic reactivity of the oxygen-related DU, a chemical feature that determines the biochemical behavior towards bioactive sites. The majority of biological macromolecules (nucleic acids, proteins) are nucleophilic. For example, in proteins, accessible thiol and primary amino groups constitute strongly nucleophilic centers. Chemical modification of these nucleophilic sites often alters or decreases protein function, resulting in cytotoxicity.[32] Therefore, a measure of the presence of carbonyls/epoxides in aerosol particles might assist in the prediction of electrophilic stress induced by airborne particle-bound chemicals. Otherwise, oxygen-rich organics in SOA with no or a low contribution of carbonyl/epoxide functionalities suggests that the oxygen is present in the peroxide form, potentially increasing in this case oxidative stress and causing disruptions in normal mechanisms of cellular signaling leading to many pathophysiological conditions. Since the awareness of health effects of particulate matter is increasing, knowledge about the potential carbonyl/epoxide contribution or its absence could help to understand physiological impacts of atmospheric particulate matter.[33]

For the above-mentioned reasons, we suggest a new metric – the maximum carbonyl ratio (MCR) – which describes the maximal contribution of carbonyl/epoxide functionalities in individual molecules composing organic aerosols, that can be directly derived from HRMS datasets. It should be clearly noted here that the proposed MCR is meant as a metric for the interpretation of mass spectrometry datasets in which hundreds to thousands of compounds are identified. Similar to other metrics that have been successfully used in the interpretation of HRMS data (e.g., DBE, AI), a calculated MCR value of a single molecular formula is not unequivocal evidence of the presence of carbonyl functionalities. Applied to a variety of compounds, however, the presented metric can be useful to visualize and interpret results on the chemical composition of complex, oxygen-rich multifunctional mixtures such as atmospheric SOA. Actually, based on the discussion above the suggested metric should be named 'maximum carbonyl/epoxide ratio'. However, it is generally assumed that the contribution of epoxides to SOA is low[34,35] and therefore most of the DU introduced by oxygen functionalities in connection with SOA formation can be expected to result from carbonyl groups. Consequently, from now on just the terms 'carbonyls' or 'carbonyl ratio' are used for convenience instead of 'carbonyl/epoxide' when we refer to the DU by oxygen functionalities. Nevertheless, atmospheric chemical interest in epoxy chemistry has recently increased considerably, especially in connection with isoprene chemistry and the formation of organosulfates.[36,37] But also the very high electrophilicity of epoxides, and thus their high toxic potency, means that the contribution of epoxides to the MCR value should not be ignored. The purpose of this paper is to introduce MCR as a new metric for the analysis of HRMS data and to present it in combination with Van Krevelen diagrams as a visualization tool (MCR-VK diagrams) to achieve a better categorization of complex ambient OA samples. The validation and applicability of the MCR-VK diagram are tested by applying the concept to selected samples of ambient organic aerosols and a few samples from laboratory-generated SOA.

2 | MATERIALS AND METHODS

2.1 | Laboratory SOA generation and collection

SOA was formed from the ozonolysis and photooxidation of selected VOCs without the addition of seed aerosol in a 7 L quartz flow tube.[38] Ozonolysis was performed by mixing α-pinene in the flow tube with ozone. The concentrations of the SOA precursor were adjusted in the range between 400 and 700 ppb and the O_3 concentrations were between 980 and 1100 ppb. Isoprene SOA was generated in a 33 L smog chamber through gas-phase photooxidation of the SOA precursor. The isoprene concentration was adjusted in the range between 300 and 500 ppb and the concentration of OH radicals during the experiments was estimated to be $\sim 5.2 \times 10^{11}$ cm^{-3}. A Scanning Mobility Particle Sizer (SMPS; GRIMM Aerosol Technik GmbH & Co. KG, Ainring, Germany) was used to measure the number and size distribution of the formed SOA particles. SOA was collected on 47 mm Omnipore Teflon filters (100 nm pore size; Merck Chemicals GmbH, Darmstadt, Germany).

2.2 | Ambient PM sampling

The 24-h integrated PM samples were collected at the SMEAR II station in Hyytiälä, a boreal forest monitoring station in Finland, and at a central urban site in Beijing[7] (China). A three-stage Dekati PM10 impactor (Pallflex Tissuquartz 2500QAT-UP) was used for the boreal forest samples collected from 17–19 July 2017. The sampling flow rate through the sampler was set to 35 L min^{-1}. The fine particle mode (<1 μm) was collected on Teflon filters (PALL, 47 mm diameter).

The samples from Beijing were collected from January 7 to 9, 2014, on prebaked quartz fiber filters (8 × 10 in) using a large volume sampler (Tisch, Cleveland, OH, USA) at a flow rate of 1050 L min^{-1}. All filters were stored in glass vials at −20°C or −80°C until analysis.

2.3 | Sample preparation and HRMS analysis

The analysis of the filter samples was carried out at the Johannes Gutenberg-University in Mainz, Germany. Parts of the filters were extracted twice with 1.5 mL methanol in an ultrasonic bath for 30 min. After insoluble particles had been removed by a 0.2 μm Teflon filter, the extracts were evaporated to dryness under a gentle nitrogen stream. Finally, the extracts were dissolved with a variable volume of an acetonitrile/water mixture (1:9, v/v) to adjust the particle mass concentration between 150 and 400 μg/mL.

The filter extract solution was then analyzed by an ultrahigh-performance liquid chromatography (UHPLC) system (Dionex UltiMate 3000; Thermo Scientific, Germany) coupled to a Q Exactive Hybride-Quadrupole-Orbitrap mass spectrometer (Thermo Scientific, Germany) (UHPLC/Orbitrap MS). The detailed description of the UHPLC/Orbitrap MS method can be found in our previous study.[7] In brief, analytes were separated using a Hypersil Gold C18 column (50 × 2.0 mm, 1.9 μm particle size; Thermo Scientific, Germany) with the mobile phase consisting of (A) ultrapure water with 2% acetonitrile and 0.04% formic acid and (B) acetonitrile with 2% ultrapure water. The gradient elution was performed by the A/B mixture at a total flow rate of 500 μL/min as follows: 0–1.5 min 2% B, 1.5–2.5 min from 2% to 20% B, 2.5–5.5 min 20% B, 5.5–6.5 min from 20% to 30% B, 6.5–7.5 min from 30% to 50% B, 7.5–8.5 min from 50% to 98% B, 8.5–11.0 min 98% B, 11.0–11.05 min from 98% to 2% B, 11.05–11.1 min 2% B. The Q Exactive Orbitrap mass spectrometer was equipped with a heated ESI source at 120°C, using a spray voltage of −3.3 kV for the negative ion mode. The mass resolution power was 70,000 at *m/z* 200 and the mass scanning range was set to *m/z* 80–500.

2.4 | Data processing

The data obtained from UHPLC/Orbitrap MS were analyzed by an open-source software for mass spectrometry data processing with the main focus on LC/MS data (MZmine 2.37). The detailed processing steps and parameters in the software are shown in the supporting information. The output of MZmine data includes *m/z* ratios, formulas, retention times and peak areas of detected organic compounds. Molecular formulas were expressed as $C_CH_HO_ON_NS_S$, where the subscript characters $_C$, $_H$, $_O$, $_N$ and $_S$ correspond to the numbers of carbon, hydrogen, oxygen, nitrogen and sulfur atoms in the molecular formula. To remove chemically unreasonable formulae, identified assignments were constrained by setting H/C, O/C, N/C and S/C ratios in the ranges of 0.3–3, 0–3, 0–1.3 and 0–0.8, respectively.[7]

3 | RESULTS AND DISCUSSION

3.1 | Definition of maximum carbonyl ratio (MCR)

It is recognized that the structral characteristics of organic molecules in aerosols are essential for the evaluation of their behavior and their environmental interactions, i.e., chemical reactivity, vapor pressure, interaction with water or biological activity. A central metric, which can be directly calculated from the elemental composition, is the number of double bonds in a molecule (double-bond equivalent (DBE) also named degree of unsaturation (DU)). The DBE is calculated assuming that all atoms obey the octet rule (except for hydrogen) and that the DU is caused by covalent bonds between carbons. For $C_CH_HO_ON_NS_S$ compounds the DBE can than be expressed as:

$$\mathrm{DBE} = 1 + \mathrm{C} - 0.5\mathrm{H} + 0.5\mathrm{N} \quad (1)$$

Based on this definition, the DBE describes the number of C–C multiple bonds plus rings in a molecule and is a well-established metric to assess the DU of molecules obtained by mass spectrometry. By its definition the DBE is thus independent of the number of O and S atoms, which results in a potential overestimation of the number of C–C double/triple bonds in O/S-containing molecules. Therefore, the aromaticity index (AI) and the aromaticity equivalent (Xc) were introduced, which also consider the influence of O and S on the DU:

$$\mathrm{AI} = \frac{\mathrm{DBE(AI)}}{\mathrm{C(AI)}} = \frac{1 + \mathrm{C} - \mathrm{O} - \mathrm{S} - 0.5(\mathrm{N} + \mathrm{H})}{\mathrm{C} - \mathrm{O} - \mathrm{S} - \mathrm{N}} \quad (2)$$

(for $C_CH_HO_ON_NS_S$ compounds[25])

$$\mathrm{Xc} = \frac{(\mathrm{C} - m\mathrm{O}) - [(\mathrm{H} - \mathrm{N}) - (\mathrm{C} - m\mathrm{O})]}{\mathrm{DBE} - m\mathrm{O}} + 1 \quad (3)$$

(for $C_CH_HO_ON_N$ compounds; *m* is the fraction of oxygen atoms involved in π-bond structure of the compound[24])

The AI reflects the C–C double-bond density in a molecule including the possibility that heteroatoms can also form double bonds; the Xc further refines this concept by making it independent from the degree of alkylation. In principle, both indices are minimum criteria for the presence of aromatics and condensed aromatics in the sample material by correcting the DBE assuming contributions from heteroatom π-bond structures, such as C=O- or S=O-containing functionalities. Both parameters are succesfully used for the characterization of natural organic matter or mineral oils and have been proved to represent a step towards structural identificaiton of complex organic mixtures. The concept presented here follows a similar approach, but now by estimating a maximum criterion for the presence of carbonyl functionalities. This is done first for pure CHO compounds, often the largest group of organic compounds in atmospheric aerosol particles. A simple distinction of the cases is the basis for the MCR definition. When the number of oxygen atoms *O* in

a $C_CH_HO_O$ compound is larger or equals the DBE of this compound ($O \geq$ DBE), then the MCR is calculated as:

$$MCR = \frac{DBE}{O} \quad (4)$$

Or, in other words, it is assumed that in case unsaturation is observed, all oxygen atoms contribute to it (i.e., the molecule's unsaturation is only contributed by O atoms by forming the carbonyl group and all *O* atoms are part of a C=O functionality). For example, for $C_2H_2O_2$ (DBE = 2), the MCR is 1 (e.g., glyoxal), for $C_2H_4O_2$ (DBE = 1) the MCR is 0.5 (e.g., glycolaldehyde) and for $C_2H_6O_2$ (DBE = 0) the MCR is zero (e.g., glycol). If the number of oxygen atoms in the molecule is smaller than its DBE value ($O <$ DBE), then the MCR is considered to equal 1 (i.e. all oxygen atoms contribute to the DBE), again the maximum criteria for the presence of carbonyl functionalities. In this case all of the oxygen atoms are assumed in the form of a carbonyl group (e.g., aldehydes or ketones). Thus, the MCR is a metric to predict the possible maximum of carbonyl groups in the molecules.

3.2 | MCR-VK diagram

Motivated by the capabilities of HRMS in combination with soft ionization techniques to observe protonated or deprotonated molecules and directly assign thousands of elemental compositions, a useful concept was recently introduced which is named the "compositional space of molecules".[39] It represents the isomer-filtered complement of the entire space of molecular structures based on a given elemental composition, e.g., $C_CH_HO_O$. The compositional space is defined by the laws of chemical binding and is typically restricted to a certain mass range. This concept was also used here to relate the variety of observed organic aerosol components to all possible CHO compounds within the framework of VK diagrams. Consequently, an artificial dataset was constructed which comprises all theoretical $C_CH_HO_O$ molecular formulae for CHO compounds with up to 15 carbon atoms. To further explore the resulting chemical space the MCR values of all individual compound were calculated as described above.

In Figure 1, the dots represent the C,H,O-compositional space of molecules within the molecular H/C range between 0–2.5 and O/C range between 0 and 1.2. The different gray scale colors relate to defined MCR ranges based on the theoretically possible functionalities of the underlying chemical components. The white dots represent all compounds in the MCR range between 0 and 0.2 and include compounds without any carbonyl functionality (MCR = 0), i.e., completely saturated compounds, up to compounds in which 20% of the oxygen atoms can be present in a carbonyl functionality. Aiming on a practical categorization system we introduce three threshold lines (A, B, C; see Figure 1). Compounds between lines A and B possess MCR values in the range 0.2–0.5, compounds between lines B and C have MCR values in the range 0.5–0.9, and compounds below line C have values in the range 0.9–1.0. This means that, for example, compounds located above line A either contain no carbonyl functionalilties or a maximum of 20% of the oxygen atoms can be carbonyl oxygen (C=O), the majority (80–100%) of the oxygens within these compounds has to be single-bound hydroxyl (R-OH), hydroperoxy (R-OOH), ether (R-O-R) or peroxy oxygen (R-OO-R). In contrast, in compounds appearing below line C in the VK diagram, 90% of the unsaturation can be present in the form of carbonylic oxygen. As in the case of AI and Xc, one cannot read a certain chemical functionality from the position of a dot (e.g., number of carbonyl O or number of aromatic rings), the MCR parameter is simply a limit value consideration to better structure the VK diagram in a region that is not covered by AI or Xc.

To get an idea about potential candidates contributing to the different areas in the MCR-VK diagram, lines A, B and C shown in Figure 1 are also depicted in Figure 2, where selected typical SOA

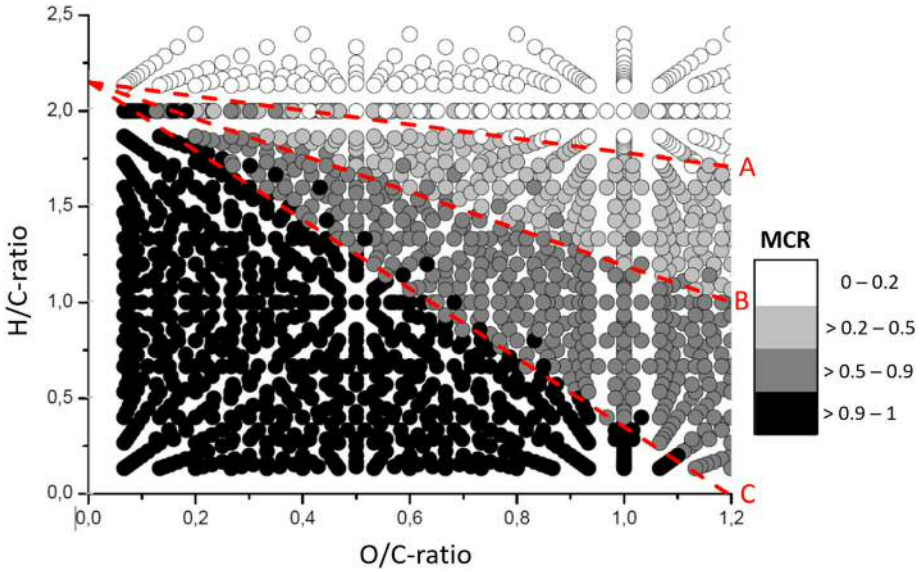

FIGURE 1 MCR-VK diagram of all possible CHO subgroups with up to 15 carbon numbers. The different colors indicate the value of the maximum carbonyl ratio (MCR). The dashed lines (A, B and C) represent different boundaries for a practicable categorization of SOA CHO compounds

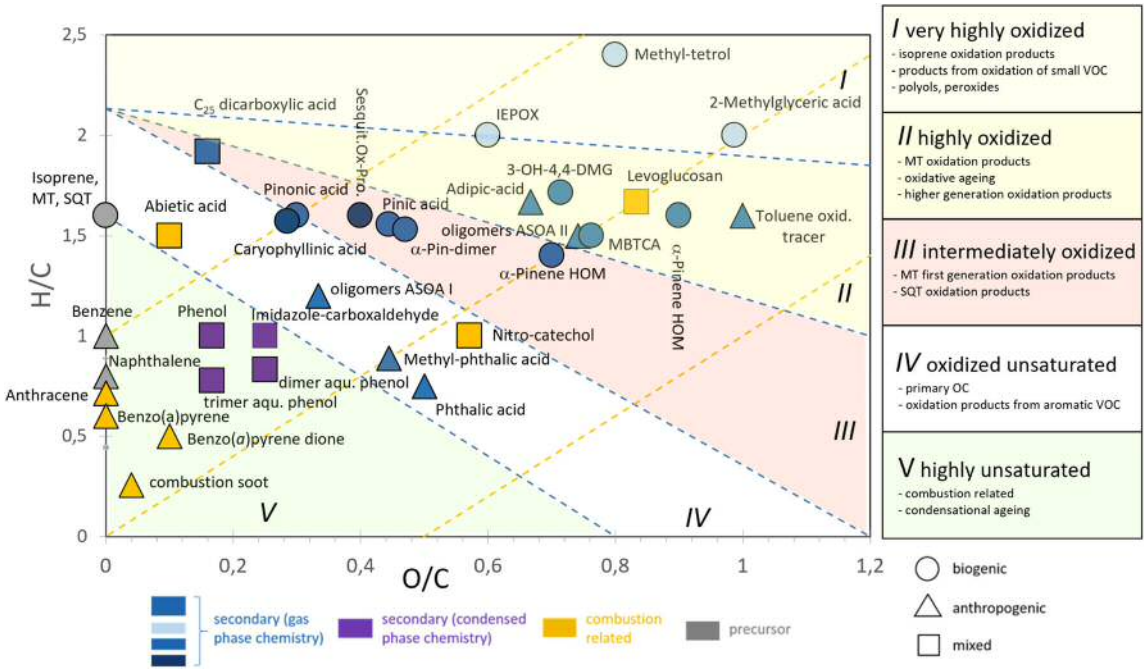

FIGURE 2 MCR-VK diagram of well-known organic marker compounds, which are defined as different colors and shapes according to their source and functionality. MCR-VK diagram was divided into five areas: I for very highly oxidized organic compounds (VHOOCs), II for highly oxidized organic compounds (HOOCs), III for intermediately oxidized organic compounds (IOOCs), IV for oxidized unsaturated organic compounds (OUOCs) and V for highly unsaturated organic compounds (HUOCs). As additional information the green dotted lines show the carbon oxidation state

precursors and SOA compounds are shown.[40–68] The molecular formulas, structures, DBE values, MCR values and suggested precursors of the selected marker molecules are listed in Table S1 (supporting information). SOA compounds formed from gas-phase chemistry are colored in blue, compounds which are known to be formed from condensed-phase chemistry are represented in purple, while a selection of marker compounds related to combustion processes are yellow-colored and a selection of SOA precursors are colored in grey. The biogenic SOA markers generated from gas-phase chemistry are further divided based on their origin from isoprene (light blue), monoterpene (MT, blue) or sesquiterpene (SQT, dark blue) oxidation. The shape of the data points indicates whether the specific marker is mainly biogenic (circles), anthropogenic (triangle) or from mixed sources (square).

Although definitely the data points scatter within the MCR-VK diagram, a certain structure is visible. Most of the typical SOA compounds are located in the areas I, II and III, defined by the MCR as explained above. For example, isoprene particle-phase oxidation products show up in area I, which generally includes products from the oxidation of smaller VOCs. Several MT and SQT first-generation products (e.g., pinic acid) are located in area III, while higher generation oxidation products, such as MBTCA or highly oxygenated organic molecules (HOMs), which are formed by multiple oxidation steps, are preferentially located in area II.[69–71] These observations can be explained by the well-known gas/particle partitioning behavior of the products: Smaller VOC precursors, such as the C_5 hydrocarbon isoprene, have to undergo multiple oxidation steps and the introduction of more oxygen-containing functionalities before the vapor pressure of the products enables them to partition into the particle phase. Several of the atmospheric gas-phase oxidation mechanisms not only introduce oxygen (shifting the molecules to the right along the x-axis in the VK diagram) and use up unsaturation of C–C double bonds or cyclic structures, but also introduce hydrogen (reaction with HO_2, hydrolysis), shifting the products up in the VK diagram. However, when the SOA precursor is a larger VOC, exemplified here by MT- or SQT-derived SOA, the products will partition into the particle phase much earlier, i.e., not necessarily have to undergo multiple oxidation steps before they enter the particle phase. Nevertheless, a certain degree of chemical aging still proceeds, shifting these products from area III into area II. To name the described areas more specifically, we characterize them as very highly oxidized organic compounds (VHOOCs) (area I), highly oxidized organic compounds (HOOCs) (area II) and intermediately oxidized organic compounds (IOOCs) (area III). In addition, according to the degree of unsaturation and oxygen content, the MCR-VK diagram in Figure 2 is further differentiated into the areas IV and V. Within area IV, named oxidized unsaturated organic compounds (OUOCs), primarily released aromatic OA components and oxidation products from aromatic VOCs are located, compounds which still contain aromatic ring structures. Finally, in area V condensed aromatic structures are showing up, including polycyclic aromatic hydrocarbons (PAHs) or oxygen-

containing PAHs, defined here as highly unsaturated organic compounds (HUOCs). In this region most of the oxygen atoms are suggested to be present in the form of carbonyl oxygen. These combustion-related compounds are able to explain the observed very low H/C ratios. Another group of compounds which might contribute to area V are products from aqueous phase chemistry, for example, of phenolic compounds or glyoxal heterogeneous chemistry.[57,72] However, there is no doubt that the MCR value loses meaningfulness in regions IV and V, but here the use of the aromatic indices AI and Xc already introduced above helps to further categorize the CHO compounds localized in these areas (see also Figure 3).

3.3 | MCR-VK diagram application on aerosol samples

To test the usefulness or limitations of the proposed MCR concept and MCR-VK diagrams in the analysis of complex atmospheric aerosol samples, we analyzed the chemical composition of SOA samples from both laboratory experiments and field measurements. The chemical composition of the samples was measured by UHPLC combined with ESI Orbitrap MS as described above.

The MCR-VK diagrams from samples of laboratory α-pinene and isoprene SOA, as well as of field samples from Hyytiälä and Beijing, are shown in Figure 3. It should be noted that in Figure 3 only compounds consisting of carbon, hydrogen and oxygen atoms (CHO compounds) are presented. The size of the dots in Figure 3 are logarithmically scaled by the fourth root of the peak area of the respective CHO compounds and the colors are selected based on the Xc value (with $0 \le Xc < 2.5$ (grey), $2.5 \le Xc < 2.7143$ (purple) and $Xc \ge 2.7143$ (red), background colors of areas of I–V are the same as in Figure 2).

Figure 3a shows particle-phase α-pinene SOA composition depicted in an MCR-VK diagram. The largest fraction (53%) of α-pinene SOA components is located in area III, while only a few compounds show up in area I. This observation indicates that most SOA products from ozone-oxidation of α-pinene are carbonyl oxygen-containing compounds with MCR values of 0.5–0.9 and only a few of them are pure hydroxyl or peroxide oxygen-containing compounds with MCR values between 0–0.2. Since these laboratory flow tube experiments allowed only a low level of further oxidation processes, the aerosol consists mainly of first-generation oxidation products of the monoterpene. The blue dot in Figure 3a is taken from a study by Claflin et al[73] in which a combination of derivatization and spectrophotometric methods was

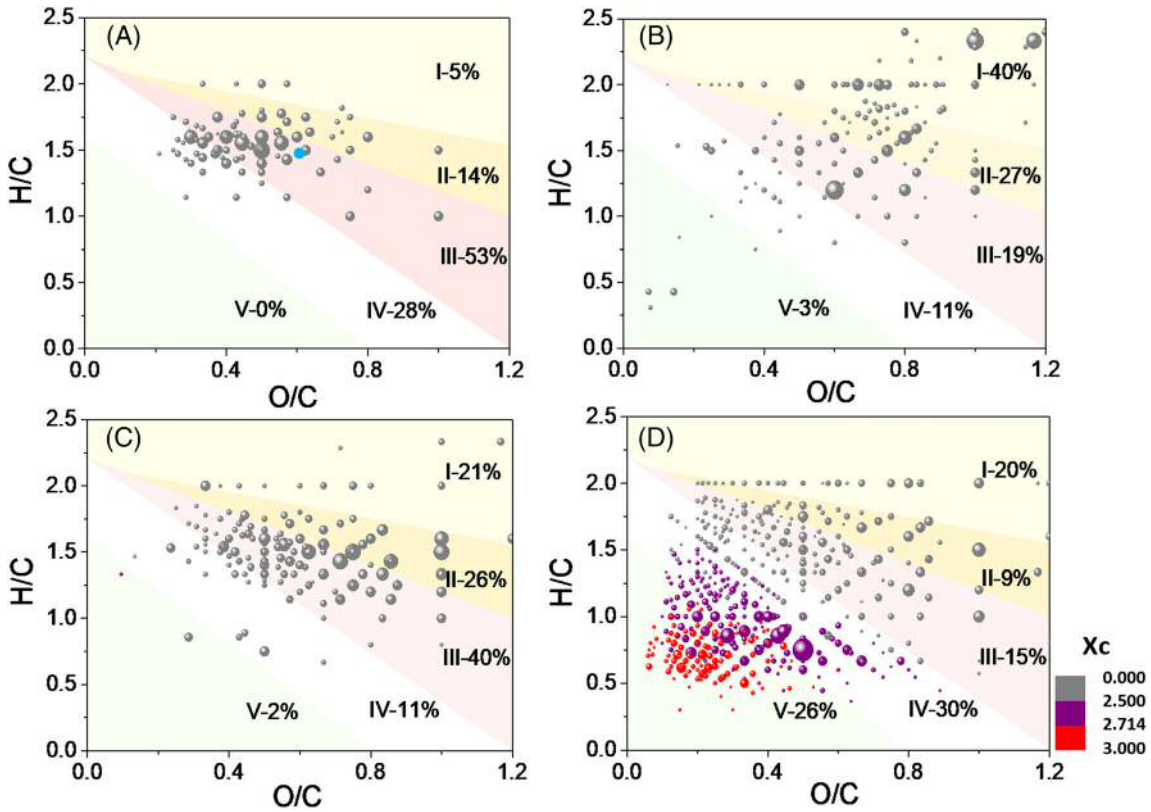

FIGURE 3 MCR-VK diagrams of α-pinene ozonolysis SOA (a), isoprene photooxidation SOA (b), Hyytiälä OA (c) and Beijing OA (d). The size of the bubbles indicates the fourth root of the intensity of each compound and the colors correspond to the Xc value. The blue dot in (a) shows the results of Claflin et al,[73] who studied functional group composition of SOA formed from ozonolysis of α-pinene under similar experimental conditions

used to quantify peroxide, carbonyl, carboxyl, ester, and hydroxyl groups to examine the α-pinene/ozone SOA composition, actually under similar experimental conditions. Although completely different analytical methods were used and, of course, only one data point is available on the total composition, the results of the study by Claflin et al are not only roughly in the center of the data shown here (they report average O/C an H/C ratios), but the [carbonyl-O] to [total-O] ratio of 0.56 calculated by Claflin et al also fits well with the MCR concept as presented here.[73] Figure 3b shows the MCR-VK diagram of SOA products from isoprene reacted with OH radicals. As can be seen in the figure, the distribution of products generated from α-pinene and isoprene to areas I–V are quite different. Isoprene SOA products span over a considerably larger region of the MCR-VK diagram than the α-pinene SOA products. Most isoprene SOA products (40%) show up in area I, clearly demonstrating that these compounds are VHOOCs with a very low MCR value (0–0.2) and that the majority of oxygen functionalities are presented in the form of non-carbonyl groups (e.g., OH and OOH). This observation agrees well with the fact that large amounts of diols, tetrols and hydroperoxides were identified in isoprene-derived SOA in previous studies.[74] Figures 3c and 3d show MCR-VK diagrams for ambient aerosol samples. Figure 3c, which shows the results of the LC/MS analysis of aerosol field samples from Hyytiälä, indicates a similar aerosol composition as in the case of α-pinene SOA (Figure 3a). The largest fraction (40%) of the compounds is located in area III, followed by areas II (26%), I (21%), IV (11%) and V (2%). The observed similarity can be explained by the fact that at this measurement site monoterpenes are the primary source of SOA and α-pinene is one of the most important individual monoterpenes released at this site. Also previous studies have shown that the photooxidation and ozonolysis of biogenic VOCs contribute to the major fraction of aerosol components in Hyytiälä.[75–77] However, compared with the laboratory α-pinene SOA shown in Figure 3a, significantly more particle-phase products in areas I and II were observed, indicating that the particles in the ambient atmosphere experienced more intensive oxidation processes and oxidative ageing compared with laboratory α-pinene SOA. Finally, Figure 3d shows the application of an MCR-VK diagram on the Beijing aerosol samples, certainly a location with very different atmospheric conditions compared with the boreal forest station. The majority of Beijing particle-phase compounds are located in the highly unsaturated and less oxidized region of the MCR-VK diagram, i.e., areas IV (30%) and V (26%). As already discussed above, the indication of the presence of OUOCs (IV) and HUOCs (V), which mostly contain aromatic structures with low degrees of oxidation, is probably related to combustion processes.[7] The numerical comparison yields, 20%, 9% and 15%, of Beijing aerosol products are located in areas I (VHOOCs), II (HOOCs) and III (IOOCs), respectively, indicating that also in Beijing samples there is a significant contribution from oxidative processing of SOA components and probably SOA generated by biomass burning.[78,79]

4 | CONCLUSIONS

The maximum carbonyl ratio (MCR) is a metric that can be used to estimate the contribution of carbonyl groups in a molecule. According to the MCR value, the maximum number of carbonyl groups in molecules can be quantified. Furthermore, an updated visualization tool, the MCR-VK diagram, is developed by the combination of the MCR value and a traditional VK diagram. By locating selected typical SOA compounds within the MCR-VK diagram, five areas were defined referring to very highly oxidized organic compounds (area I, VHOOCs), highly oxidized organic compounds (area II, HOOCs), intermediately oxidized organic compounds (area III, IOOCs), oxidized unsaturated organic compounds (area IV, OUOCs) and highly unsaturated organic compounds (area V, HUOCs), to better understand the structural information of SOA compounds in terms of the carbonyl functional group. The MCR-VK diagram approach was tested and validated using laboratory-generated SOA from ozonolysis of α-pinene, photooxidation of isoprene and ambient aerosol samples collected in Hyytiälä (boreal forest) and Beijing (megacity). Distinct distributions in the MCR-VK diagram were observed in the various aerosol samples and the comparison between them can improve the characterization of organic aerosol samples, especially an improved understanding of SOA sources and formation pathways. In summary, the use of the MCR concept or the application of MCR-VK diagrams can help to better understand the sources and the processing of atmospheric OA components based on HRMS data. As discussed above, the MCR might also prove useful for the evaluation of health-related effects of organic aerosols, since the MCR contains information about the presence of electrophilic particle-bound multifunctional organics (larger MCR values) or the presence of highly oxidized non-carbon-containing organics (low MCR values), such as (hydro)peroxides, inducing oxidative stress in the respiratory system. Although oxidative and electrophilic stress are linked, the biological pathways causing the adverse health effects of particulate air pollution are poorly understood and there is no conclusive evidence as to which particle properties are causing their toxicity. Chemical components in the particle phase are likely a key factor, but are difficult to accurately define. The suggested MCR value, easily extracted from HRMS data, might be a valuable tool to identify health-relevant particle parameters, components and sources, information which is crucial for improved and efficient air pollution mitigation strategies. In future work, the combination of MCR or MCR-VK diagrams and other metrics such as AI, Xc and carbon oxidation states (OSc) could be further used to better understand the composition, origin, history and effects of complex organic aerosols.

ACKNOWLEDGMENTS

This work was funded by the Deutsche Forschungsgemeinschaft (DFG, HO 1748/19-1, HO 1748/20-1), the German Federal Ministry of Education and Research (BMBF contract 01LK1602D), the Max Planck Society and the National Natural Science Foundation of China (NSFC) (Grant No. 41925015). Kai Wang and Yun Zhang acknowledge scholarships from the Chinese Scholarship Council (CSC). Kai Wang

acknowledges a scholarship from the Max Plank Graduate Center with Johannes Gutenberg University of Mainz (MPGC). The authors acknowledge stimulating exchange with Ulrich Pöschl.

PEER REVIEW

The peer review history for this article is available at https://publons.com/publon/10.1002/rcm.9113.

DATA AVAILABILITY STATEMENT

Data available on request from the authors.

ORCID

Yun Zhang https://orcid.org/0000-0003-4120-7203
Kai Wang https://orcid.org/0000-0002-1305-6789
Haijie Tong https://orcid.org/0000-0001-9887-7836
Ru-Jin Huang https://orcid.org/0000-0002-4907-9616
Thorsten Hoffmann https://orcid.org/0000-0003-0939-271X

REFERENCES

1. Kroll JH, Donahue NM, Jimenez JL, et al. Carbon oxidation state as a metric for describing the chemistry of atmospheric organic aerosol. *Nat Chem*. 2011;3(2):133-139.
2. Jimenez JL, Canagaratna MR, Donahue NM, et al. Evolution of organic aerosols in the atmosphere. *Science*. 2009;326(5959):1525-1529.
3. Hallquist M, Wenger JC, Baltensperger U, et al. The formation, properties and impact of secondary organic aerosol: Current and emerging issues. *Atmos Chem Phys*. 2009;9(14):5155-5236.
4. Pöschl U. Atmospheric aerosols: Composition, transformation, climate and health effects. *Angew Chem Int Ed*. 2005;44(46):7520-7540.
5. Pöschl U, Shiraiwa M. Multiphase chemistry at the atmosphere-biosphere interface influencing climate and public health in the anthropocene. *Chem Rev*. 2015;115(10):4440-4475.
6. Seinfeld JH, Pandis SN. *Atmospheric chemistry and physics: From air pollution to climate change*. 3rded. Hoboken, NJ: Wiley; 2016.
7. Wang K, Zhang Y, Huang R-J, Cao J, Hoffmann T. UHPLC-Orbitrap mass spectrometric characterization of organic aerosol from a central European city (Mainz, Germany) and a Chinese megacity (Beijing). *Atmos Environ*. 2018;189:22-29.
8. Huang RJ, Cao J, Chen Y, et al. Organosulfates in atmospheric aerosol: Synthesis and quantitative analysis of PM2.5 from Xi'an, northwestern China. *Atmos Meas Tech*. 2018;11(6):3447-3456.
9. Glasius M, Bering MS, Yee LD, et al. Organosulfates in aerosols downwind of an urban region in Central Amazon. *Environ Sci Process Impacts*. 2018;20(11):1546-1558. https://doi.org/10.1039/c8em00413g
10. Daellenbach KR, Kourtchev I, Vogel AL, et al. Impact of anthropogenic and biogenic sources on the seasonal variation in the molecular composition of urban organic aerosols: A field and laboratory study using ultra-high-resolution mass spectrometry. *Atmos Chem Phys*. 2019;19(9):5973-5991. https://doi.org/10.5194/acp-19-5973-2019
11. Tong H, Kourtchev I, Pant P, et al. Molecular composition of organic aerosols at urban background and road tunnel sites using ultra-high resolution mass spectrometry. *Faraday Discuss*. 2016;189:51-68.
12. Lin P, Yu JZ, Engling G, Kalberer M. Organosulfates in humic-like substance fraction isolated from aerosols at seven locations in East Asia: A study by ultra-high-resolution mass spectrometry. *Environ Sci Technol*. 2012;46(24):13118-13127.
13. Glasius M, Hansen AMK, Claeys M, et al. Composition and sources of carbonaceous aerosols in northern Europe during winter. *Atmos Environ*. 2018;173:127-141. https://doi.org/10.1016/j.atmosenv.2017.11.005
14. Song J, Li M, Jiang B, Wei S, Fan X, Peng P'. Molecular characterization of water-soluble humic like substances in smoke particles emitted from combustion of biomass materials and coal using ultrahigh-resolution electrospray ionization Fourier transform ion cyclotron resonance mass spectrometry. *Environ Sci Technol*. 2018;52(5):2575-2585.
15. Wang K, Zhang Y, Huang RJ, et al. Molecular characterization and source identification of atmospheric particulate organosulfates using ultrahigh resolution mass spectrometry. *Environ Sci Technol*. 2019;53(11):6192-6202.
16. Hoffmann T, Huang RJ, Kalberer M. Atmospheric analytical chemistry. *Anal Chem*. 2011;83(12):4649-4664. https://doi.org/10.1021/ac2010718
17. Noziere B, Kalberer M, Claeys M, et al. The molecular identification of organic compounds in the atmosphere: State of the art and challenges. *Chem Rev*. 2015;115(10):3919-3983.
18. Kim S, Kramer RW, Hatcher PG. Graphical method for analysis of ultrahigh-resolution broadband mass spectra of natural organic matter, the Van Krevelen diagram. *Anal Chem*. 2003;75(20):5336-5344.
19. Sleighter RL, Hatcher PG. The application of electrospray ionization coupled to ultrahigh resolution mass spectrometry for the molecular characterization of natural organic matter. *J Mass Spectrom*. 2007;42(5):559-574.
20. Hockaday WC, Purcell JM, Marshall AG, Baldock JA, Hatcher PG. Electrospray and photoionization mass spectrometry for the characterization of organic matter in natural waters: A qualitative assessment. *Limnol Oceanogr Methods*. 2009;7:81-95.
21. Hughey CA, Hendrickson CL, Rodgers RP, Marshall AG. Kendrick mass defect spectrum: A compact visual analysis for ultrahigh-resolution broadband mass spectra. *Anal Chem*. 2001;73(19):4676-4681.
22. Kendrick E. A mass scale based on $CH_2 = 14.0000$ for high resolution mass spectrometry of organic compounds. *Anal Chem*. 1963;35:2146-2154.
23. Barrow MP, Headley JV, Peru KM, Derrick PJ. Data visualization for the characterization of naphthenic acids within petroleum samples. *Energy Fuel*. 2009;23(5):2592-2599.
24. Yassine MM, Harir M, Dabek-Zlotorzynska E, Schmitt-Kopplin P. Structural characterization of organic aerosol using Fourier transform ion cyclotron resonance mass spectrometry: Aromaticity equivalent approach. *Rapid Commun Mass Spectrom*. 2014;28(22):2445-2454.
25. Koch BP, Dittmar T. Erratum: From mass to structure: An aromaticity index for high-resolution mass data of natural organic matter. *Rapid Commun Mass Spectrom*. 2016;30(1):250-250. https://doi.org/10.1002/rcm.7433
26. Ziemann PJ, Atkinson R. Kinetics, products, and mechanisms of secondary organic aerosol formation. *Chem Soc Rev*. 2012;41(19):6582-6605. https://doi.org/10.1039/c2cs35122f
27. Bianchi F, Kurten T, Riva M, et al. Highly oxygenated organic molecules (HOM) from gas-phase autoxidation involving peroxy radicals: A key contributor to atmospheric aerosol. *Chem Rev*. 2019;119(6):3472-3509. https://doi.org/10.1021/acs.chemrev.8b00395
28. Carslaw KS, Gordon H, Hamilton DS, et al. Aerosols in the pre-industrial atmosphere. *Curr Clim Change Rep*. 2017;3(1):1-15. https://doi.org/10.1007/s40641-017-0061-2
29. Verma V, Fang T, Xu L, et al. Organic aerosols associated with the generation of reactive oxygen species (ROS) by water-soluble PM2.5. *Environ Sci Technol*. 2015;49:4646-4656. https://doi.org/10.1021/es505577w

30. Tong H, Lakey PSJ, Arangio AM, et al. Reactive oxygen species formed by secondary organic aerosols in water and surrogate lung fluid. *Environ Sci Technol*. 2018;52:11642-11651. https://doi.org/10.1021/acs.est.8b03695
31. Rudich Y, Donahue NM, Mentel TF. Aging of organic aerosol: Bridging the gap between laboratory and field studies. *Annu Rev Phys Chem*. 2007;58(1):321-341. https://doi.org/10.1146/annurev.physchem.58.032806.104432
32. Zimniak P. Relationship of electrophilic stress to aging. *Free Radical Biol Med*. 2011;51(6):1087-1105. https://doi.org/10.1016/j.freeradbiomed.2011.05.039
33. Schwöbel JAH, Koleva YK, Enoch SJ, et al. Measurement and estimation of electrophilic reactivity for predictive toxicology. *Chem Rev*. 2011;111(4):2562-2596. https://doi.org/10.1021/cr100098n
34. Atkinson R. Gas-phase tropospheric chemistry of organic compounds: A review. *Atmos Environ*. 1991;24A:1-41.
35. Ji Y, Zhao J, Terazono H, et al. Reassessing the atmospheric oxidation mechanism of toluene. *Proc Natl Acad Sci*. 2017;114(31):8169-8174. https://doi.org/10.1073/pnas.1705463114
36. Paulot F, Crounse JD, Kjaergaard HG, et al. Unexpected epoxide formation in the gas-phase photooxidation of isoprene. *Science*. 2009;325(5941):730-733. https://doi.org/10.1126/science.1172910
37. Shrivastava M, Andreae MO, Artaxo P, et al. Urban pollution greatly enhances formation of natural aerosols over the Amazon rainforest. *Nat Commun*. 2019;10(1):1046. https://doi.org/10.1038/s41467-019-08909-4
38. Tong H, Arangio AM, Lakey PSJ, et al. Hydroxyl radicals from secondary organic aerosol decomposition in water. *Atmos Chem Phys*. 2016;16(3):1761-1771.
39. Hertkorn N, Ruecker C, Meringer M, et al. High-precision frequency measurements: Indispensable tools at the core of the molecular-level analysis of complex systems. *Anal Bioanal Chem*. 2007;389(5):1311-1327.
40. Ramdahl T. Retene – A molecular marker of wood combustion in ambient air. *Nature*. 1983;306(5940):580-582.
41. Myoseon Jang SRM. Products of benz[a]anthracene photodegradation in the presence of known organic constituents of atmospheric aerosols. *Environ Sci Technol*. 1997;31(4):1046-1053.
42. Matthew P, Fraser KL. Using levoglucosan as a molecular marker for the long-range transport of biomass combustion aerosols. *Environ Sci Technol*. 2000;34:4560-4564.
43. Edney EO, Kleindienst TE, Jaoui M, et al. Formation of 2-methyl tetrols and 2-methylglyceric acid in secondary organic aerosol from laboratory irradiated isoprene/NO_X/SO_2/air mixtures and their detection in ambient PM2.5 samples collected in the eastern United States. *Atmos. Environ*. 2005;39(29):5281-5289.
44. Kenneth S, Docherty WW, Lim YB, Ziemann PJ. Contributions of organic peroxides to secondary aerosol formed from reactions of monoterpenes with O_3. *Environ Sci Technol*. 2005;39:4049-4059.
45. Henze DK, Seinfeld JH. Global secondary organic aerosol from isoprene oxidation. *Geophys Res Lett*. 2006;33(9):L09812.
46. Jaoui M, Lewandowski M, Kleindienst TE, Offenberg JH, Edney EO. β-Caryophyllinic acid: An atmospheric tracer for β-caryophyllene secondary organic aerosol. *Geophys Res Lett*. 2007;34(5):L05816.
47. Sakulyanontvittaya T, Helmig D, Milford J, Wiedinmyer C. Secondary organic aerosol from sesquiterpene and monoterpene emissions in the United States. *Environ Sci Technol*. 2008;42(23):8784-8790.
48. Fu P, Chen J, Barrie LA. Isoprene, monoterpene, and sesquiterpene oxidation products in the high Arctic aerosols during late winter to early summer. *Environ Sci Technol*. 2009;43(11):4022-4028.
49. Kautzman KE, Chan MN, Chan AWH, et al. Chemical composition of gas- and aerosol-phase products from the photooxidation of naphthalene. *J Phys Chem A*. 2010;114(2):913-934.
50. Surratt JD, Chan AW, Eddingsaas NC, et al. Reactive intermediates revealed in secondary organic aerosol formation from isoprene. *Proc Natl Acad Sci*. 2010;107(15):6640-6645.
51. Ding X, Wang X-M, Zheng M. The influence of temperature and aerosol acidity on biogenic secondary organic aerosol tracers: Observations at a rural site in the Central Pearl River Delta region, South China. *Atmos Environ*. 2011;45(6):1303-1311.
52. Borrás E, Tortajada-Genaro LA. Secondary organic aerosol formation from the photo-oxidation of benzene. *Atmos Environ*. 2012;47:154-163.
53. Ehn M, Kleist E, Junninen H, et al. Gas phase formation of extremely oxidized pinene reaction products in chamber and ambient air. *Atmos Chem Phys*. 2012;12(11):5113-5127.
54. Ehn M, Thornton JA, Kleist E, et al. A large source of low-volatility secondary organic aerosol. *Nature*. 2014;506(7489):476-479.
55. Kristensen K, Cui T, Zhang H, Gold A, Glasius M, Surratt JD. Dimers in α-pinene secondary organic aerosol: Effect of hydroxyl radical, ozone, relative humidity and aerosol acidity. *Atmos Chem Phys*. 2014;14(8):4201-4218.
56. Nguyen TB, Coggon MM, Bates KH, et al. Organic aerosol formation from the reactive uptake of isoprene epoxydiols (IEPOX) onto non-acidified inorganic seeds. *Atmos Chem Phys*. 2014;14(7):3497-3510.
57. Yu L, Smith J, Laskin A, Anastasio C, Laskin J, Zhang Q. Chemical characterization of SOA formed from aqueous-phase reactions of phenols with the triplet excited state of carbonyl and hydroxyl radical. *Atmos Chem Phys*. 2014;14(24):13801-13816.
58. Shen RQ, Ding X, He QF, Cong ZY, Yu QQ, Wang XM. Seasonal variation of secondary organic aerosol tracers in central Tibetan plateau. *Atmos Chem Phys*. 2015;15(15):8781-8793.
59. Zhang RCM, Huang DD, Dalleska NF, et al. Formation and evolution of molecular products in α-pinene secondary organic aerosol. *Proc Natl Acad Sci*. 2015;112(46):14168-14173.
60. González Palacios L, Corral Arroyo P, Aregahegn KZ, et al. Heterogeneous photochemistry of imidazole-2-carboxaldehyde: HO_2 radical formation and aerosol growth. *Atmos Chem Phys*. 2016;16(18):11823-11836.
61. Kurten T, Tiusanen K, Roldin P, et al. Alpha-pinene autoxidation products may not have extremely low saturation vapor pressures despite high O:C ratios. *J Phys Chem A*. 2016;120(16):2569-2582.
62. Utieyin OO. Advanced oxidation process using ozone/heterogeneous catalysis for the degradation of phenolic compounds (chlorophenols) in aqueous system. PhD thesis, Cape Peninsula University of Technology. South Africa. 2016.
63. Al-Naiema IM, Stone EA. Evaluation of anthropogenic secondary organic aerosol tracers from aromatic hydrocarbons. *Atmos Chem Phys*. 2017;17(3):2053-2065.
64. Martinsson J, Monteil G, Sporre MK, et al. Exploring sources of biogenic secondary organic aerosol compounds using chemical analysis and the FLEXPART model. *Atmos Chem Phys*. 2017;17(18):11025-11040.
65. Pecha MB. Understanding and controlling lignocellulosic pyrolysis for the production of renewable fuel and chemical precursors. PhD thesis, Washington State University, USA. 2017.
66. Tu PJ, Hall WA, Johnston MV. Characterization of highly oxidized molecules in fresh and aged biogenic secondary organic aerosol. *Anal Chem*. 2016;88(8):4495-4501.
67. Yee LD, Isaacman-VanWertz G, Wernis RA, et al. Observations of sesquiterpenes and their oxidation products in Central Amazonia during the wet and dry seasons. *Atmos Chem Phys*. 2018;18(14):10433-10457. https://doi.org/10.5194/acp-18-10433-2018
68. Zhu W, Luo L, Cheng Z, Yan N, Lou S, Ma Y. Characteristics and contributions of biogenic secondary organic aerosol tracers to PM 2.5 in Shanghai, China. *Atmos Pollut Res*. 2018;9(2):179-188.
69. Yasmeen F, Vermeylen R, Maurin N, Perraudin E, Doussin J-F, Claeys M. Characterisation of tracers for aging of α-pinene secondary

organic aerosol using liquid chromatography/negative ion electrospray ionisation mass spectrometry. *Environ Chem*. 2012; 9(3):236.

70. Wang S, Wu R, Berndt T, Ehn M, Wang L. Formation of highly oxidized radicals and multifunctional products from the atmospheric oxidation of alkylbenzenes. *Environ Sci Technol*. 2017;51(15): 8442-8449.
71. Wang S, Riva M, Yan C, Ehn M, Wang L. Primary formation of highly oxidized multifunctional products in the OH-initiated oxidation of isoprene. A combined theoretical and experimental study. *Environ Sci Technol*. 2018;52(21):12255-12264. https://doi.org/10.1021/acs.est.8b02783
72. Sun YL, Zhang Q, Anastasio C, Sun J. Insights into secondary organic aerosol formed via aqueous-phase reactions of phenolic compounds based on high resolution mass spectrometry. *Atmos Chem Phys*. 2010; 10(10):4809-4822.
73. Claflin MS, Krechmer JE, Hu WW, Jimenez JL, Ziemann PJ. Functional group composition of secondary organic aerosol formed from ozonolysis of alpha-pinene under high VOC and autoxidation conditions. *ACS Earth Space Chem*. 2018;2(11):1196-1210. https://doi.org/10.1021/acsearthspacechem.8b00117
74. Carlton AG, Wiedinmyer C, Kroll JH. A review of secondary organic aerosol (SOA) formation from isoprene. *Atmos Chem Phys*. 2009; 9(14):4987-5005.
75. Cavalli MCF, Decesari S, Emblico L, et al. Size-segregated aerosol chemical composition at a boreal site in southern Finland, during the QUEST project. *Atmos Chem Phys*. 2006;6(4):993-1002.
76. Lee A, Goldstein AH, Keywood MD, et al. Gas-phase products and secondary aerosol yields from the ozonolysis of ten different terpenes. *J Geophys Res Atmos*. 2006;111(D7):D07302.
77. Kourtchev I, Fuller S, Aalto J, et al. Molecular composition of boreal forest aerosol from Hyytiala, Finland, using ultrahigh resolution mass spectrometry. *Environ Sci Technol*. 2013;47(9):4069-4079.
78. Ding X, Zhang Y-Q, He Q-F, et al. Spatial and seasonal variations of secondary organic aerosol from terpenoids over China. *J Geophys Res Atmos*. 2016;121(24):14,661-614,678.
79. Ding X, He Q-F, Shen R-Q, et al. Spatial and seasonal variations of isoprene secondary organic aerosol in China: Significant impact of biomass burning during winter. *Sci Rep*. 2016;6:20411.

SUPPORTING INFORMATION

Additional supporting information may be found online in the Supporting Information section at the end of this article.

How to cite this article: Zhang Y, Wang K, Tong H, Huang R-J, Hoffmann T. The maximum carbonyl ratio (MCR) as a new index for the structural classification of secondary organic aerosol components. *Rapid Commun Mass Spectrom*. 2021;35: e9113. https://doi.org/10.1002/rcm.9113